This article was downloaded by: [Renmin University of China]
On: 13 October 2013, At: 10:49
Publisher: Taylor & Francis
Informa Ltd Registered in England and Wales Registered Number: 1072954 Registered office: Mortimer House, 37-41 Mortimer Street, London W1T 3JH, UK

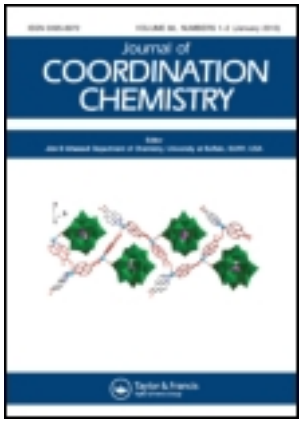

Journal of Coordination Chemistry
Publication details, including instructions for authors and subscription information:
http://www.tandfonline.com/loi/gcoo20

Hydrothermal syntheses, structures, and properties of the first examples of lanthanide 4-(4,5-diphenyl-1H-imidazol-2-yl)benzote complexes

Hui-Liang Wen [a], Wen Wen [a], Dan-Dan Li [a], Chong-Bo Liu [b] & Min He [a]

[a] State Key Laboratory of Food Science and Technology, Nanchang University, Nanchang, P.R. China

[b] School of Environment and Chemical Engineering, Nanchang Hangkong University, Nanchang, P.R. China

Accepted author version posted online: 07 Jun 2013.Published online: 08 Jul 2013.

To cite this article: Hui-Liang Wen, Wen Wen, Dan-Dan Li, Chong-Bo Liu & Min He (2013) Hydrothermal syntheses, structures, and properties of the first examples of lanthanide 4-(4,5-diphenyl-1H-imidazol-2-yl)benzote complexes, Journal of Coordination Chemistry, 66:15, 2623-2633, DOI: 10.1080/00958972.2013.812204

To link to this article: http://dx.doi.org/10.1080/00958972.2013.812204

PLEASE SCROLL DOWN FOR ARTICLE

Taylor & Francis makes every effort to ensure the accuracy of all the information (the "Content") contained in the publications on our platform. However, Taylor & Francis, our agents, and our licensors make no representations or warranties whatsoever as to the accuracy, completeness, or suitability for any purpose of the Content. Any opinions and views expressed in this publication are the opinions and views of the authors, and are not the views of or endorsed by Taylor & Francis. The accuracy of the Content should not be relied upon and should be independently verified with primary sources of information. Taylor and Francis shall not be liable for any losses, actions, claims, proceedings, demands, costs, expenses, damages, and other liabilities whatsoever or howsoever caused arising directly or indirectly in connection with, in relation to or arising out of the use of the Content.

This article may be used for research, teaching, and private study purposes. Any substantial or systematic reproduction, redistribution, reselling, loan, sub-licensing, systematic supply, or distribution in any form to anyone is expressly forbidden. Terms &

Conditions of access and use can be found at http://www.tandfonline.com/page/terms-and-conditions

Downloaded by [Renmin University of China] at 10:49 13 October 2013

Journal of Coordination Chemistry, 2013
Vol. 66, No. 15, 2623–2633, http://dx.doi.org/10.1080/00958972.2013.812204

Taylor & Francis
Taylor & Francis Group

Downloaded by [Renmin University of China] at 10:49 13 October 2013

Hydrothermal syntheses, structures, and properties of the first examples of lanthanide 4-(4,5-diphenyl-1H-imidazol-2-yl) benzote complexes

HUI-LIANG WEN*†, WEN WEN†, DAN-DAN LI†, CHONG-BO LIU‡ and MIN HE†

†State Key Laboratory of Food Science and Technology, Nanchang University, Nanchang, P.R. China
‡School of Environment and Chemical Engineering, Nanchang Hangkong University, Nanchang, P.R. China

(*Received 24 October 2012; in final form 18 April 2013*)

Three new lanthanide coordination polymers with 4-(4,5-diphenyl-1H-imidazol-2-yl)benzoic acid (H_2PA), $[Ln(HPA)_3(H_2O)_2]\cdot 2H_2O$ [Ln = Pr (**1**); Eu (**2**); Er (**3**)] were obtained by hydrothermal syntheses and characterized by single crystal X-ray diffraction, elemental analysis, IR spectroscopy, and powder X-ray diffraction. Complexes **1–3** are isomorphous 2-D supramolecular structures, in which lanthanide ions are bridged by carboxyl groups of HPA^- to form 1-D chain structures, and the chains are further linked to 2-D supramolecular structures by hydrogen bonds. HPA^- exhibit chelating and μ_2-bridging coordination mode. The thermogravimetric analysis of **2** was carried out to examine the thermal stability and the photoluminescence of **2** was investigated.

Keywords: 4-(4,5-Diphenyl-1H-imidazol-2-yl)benzoic acid; Lanthanide complexes; Supramolecular network; Hydrothermal synthesis; Photoluminescence

1. Introduction

The architecture of supramolecular networks has aroused interest due to their structural diversity and potential applications in magnetism, absorption, luminescence, and biological activity [1–6]. In particular, much attention has been focused on the design and synthesis of supramolecular coordination polymers based on multifunctional organic ligands with N- and O-donors [7–10]. Such compounds are hydrogen-bond acceptors as well as hydrogen-bond donors and good candidates for assembly of high-dimensional 3d, 4f, or 3d-4f supramolecular networks. Compounds with an imidazole ring system, such as 2,4,5-triphenylimidazole (TPI) and its derivatives, have applications such as pharmacological [11], photographic [12], electroluminescent [13], and optical materials [14–16], the result of the large conjugated-system in TPI [17]. There are a few reports on the structures of TPI and its derivatives [18, 19] and some transition metal complexes with hydroxy-substituted TPI derivatives have been characterized [20–24].

*Corresponding author. Email: hlwen70@163.com

© 2013 Taylor & Francis

Downloaded by [Renmin University of China] at 10:49 13 October 2013

However, there are no reports on carboxylic acid-substituted TPI derivatives. The harder oxygens of the carboxylic acid are expected to increase the ability of TPI to coordinate to lanthanide ions according to "soft-hard acid-base theory" [25–27]. As compared to reports on d-block transition metal ions, lanthanide supramolecular compounds are less common, because the higher coordination numbers of lanthanides make it harder to control the coordination chemistry, and thereby the expected structures of the products. However, lanthanide supramolecular compounds exhibit promising magnetic and luminescence properties as a consequence of the unique spectroscopic and electronic characteristics associated with their 4f electron configuration [28]. More interest has been given to lanthanide complexes recently [29–31].

Recently, our group prepared a series of TPI derivatives via the Radziszewski synthesis. In the present work, Pr, Eu, and Er salts were selected as representatives of light, middle, and heavy rare earth elements in the reaction with 4-(4,5-diphenyl-1H-imidazol-2-yl)benzoic acid (H_2PA) under hydrothermal conditions, in order to obtain new lanthanide coordination polymers.

2. Experimental

2.1. *Materials and physical measurements*

All materials and reagents except H_2PA [32–34] were obtained commercially and used without purification. C, H, and N elemental analyses were carried out with a Flash EA 1112 Elemental Analyzer. IR spectra were recorded with a Nicolet Avatar 360 FT-IR spectrometer from 4000–400 cm^{-1} using KBr pellets. Powder X-ray diffraction (PXRD) measurements were performed on a Bruker D8 Avance X-ray diffractometer using Cu Kα radiation ($\lambda = 1.54056$ Å) at 40 kV and 40 mA. Thermal stability studies were carried out on a Pyris diamond TGA/DTA thermal analyzer. Fluorescence measurements were made on a Hitachi FS-4500 fluorophotometer at room temperature.

2.2. *Synthesis of 1–3*

2.2.1. $[Pr(HPA)_3(H_2O)_2]\cdot 2H_2O$ (1). A mixture of 0.025 mM Pr_2O_3, 0.05 mM $CoCl_2\cdot 6H_2O$, 0.05 mM H_2PA, and 0.2 mM 0.65 M NaOH in 10 ml water was sealed in a 25 ml Teflon-lined stainless reactor and heated at 170 °C for 72 h under autogeneous pressure. The reaction mixture was then cooled to 120 °C at 10 °C/h, followed by slow cooling to room temperature, upon which the desired product appeared as light blue block-shaped crystals (2.89 mg, 4.7% yield). Anal. Calcd for $C_{66}H_{53}PrN_6O_{10}$ (1231.1): C, 64.39; H, 4.34; N, 6.82%. Found: C, 64.78; H, 4.98; N, 7.15%. IR data (KBr pellet, ν/cm^{-1}): 3436 (m) $\nu(H_2O)$, 3067 (m) ν(C–H), 1568 (*versus*) ν(C=O), 1500 (w), 1418 (m), 1250 (s), 1082 (m), 816 (m), 772 (m), 697 (w) $\nu(C_6H_6)$.

2.2.2. $[Eu(HPA)_3(H_2O)_2]\cdot 2H_2O$ (2). The synthesis of 2 was similar to that of 1 except that Eu_2O_3 and $ZnCl_2\cdot 4H_2O$ were used instead of Pr_2O_3 and $CoCl_2$, and the reaction temperature was decreased to 160 °C. Upon cooling to RT, the desired product appeared as colorless rhomboid-shaped crystals (3.95 mg, 6.4% yield). Anal. Calcd for $C_{66}H_{53}EuN_6O_{10}$ (1242.1): C, 63.81; H, 4.30; N, 6.76%. Found: C, 63.38; H, 4.46; N, 7.03%. IR data

Downloaded by [Renmin University of China] at 10:49 13 October 2013

Table 1. Crystal data and refinement parameters for **1–3**.

Complex	1	2	3
Empirical formula	$C_{66}H_{53}PrN_6O_{10}$	$C_{66}H_{53}EuN_6O_{10}$	$C_{66}H_{53}ErN_6O_{10}$
Formula weight	1231.05	1242.10	1257.40
T (K)	291(2)	291(2)	291(2)
Crystal system	Triclinic	Triclinic	Triclinic
Space group	$P\bar{1}$	$P\bar{1}$	$P\bar{1}$
a/Å	9.575(9)	9.576(6)	9.545(8)
b/Å	13.157(12)	13.243(9)	13.138(11)
c/Å	25.374(2)	25.231(17)	25.251(2)
α/°	99.961(10)	100.051(7)	100.042(10)
β/°	96.982(10)	96.909(7)	96.785(10)
γ/°	100.027(10)	100.431(7)	100.019(10)
V (Å^3)	3062.2(5)	3060.0(3)	3034.2(2)
Z	2	2	2
θ range (°)	2.44–25.50	2.43–25.50	2.45–25.50
μ (mm^{-1})	0.858	1.087	1.446
F (000)	1260	1268	1278
D_c (mg·m^{-3})	1.335	1.348	1.376
Goodness-of-fit on F^2 (e·Å^{-3})	0.998	1.013	1.025
No. data collected	22,957	22,785	19,824
No. unique data	11,316	11,285	10,950
R_{int}	0.0330	0.0297	0.0289
R_1, wR_2 [$I > 2\sigma(I)$]	0.0460, 0.1346	0.0319, 0.0855	0.0379, 0.0936
R_1, wR_2 (all data)	0.0583, 0.1440	0.0390, 0.0893	0.0470, 0.1000
Largest diff. peak and hole (e·Å^{-3})	1.442, −0.494	1.040, −0.637	1.124, −0.619

(KBr pellet, ν/cm^{-1}): 3431 (m) ν(H_2O), 3062 (m) ν(C-H), 1571 (*versus*) ν(C=O), 1503 (w), 1421 (m), 1253 (m), 1078 (m), 825 (m), 774 (m), 699 (w) ν(C_6H_6).

2.2.3. [Er(HPA)$_3$(H$_2$O)$_2$]·2H$_2$O (3). The synthesis of 3 was also similar to that of 1 except that Er_2O_3 was used instead of Pr_2O_3. Upon cooling to RT, the desired product appeared as light pink block-shaped crystals (3.01 mg, 4.8% yield). Anal. Calcd for $C_{66}H_{53}ErN_6O_{10}$ (1257.4): C, 63.04; H, 4.25; N, 6.68%. Found: C, 63.29; H, 4.37; N, 7.03%. IR data (KBr pellet, ν/cm^{-1}): 3423 (m) ν(H_2O), 3059 (m) ν(C–H), 1572 (*versus*) ν(C=O), 1503 (w), 1422 (m), 1248 (m), 1083 (m), 825 (m), 762 (m), 692 (w) ν(C_6H_6).

2.2.4. X-ray crystallography. Single crystal X-ray data of **1–3** were collected using a Bruker APEX-II area-detector diffractometer with graphite-monochromated Mo–Kα radiation ($\lambda = 0.71073$ Å). Semi-empirical absorption corrections were applied using SADABS [35]. The structures were solved by direct methods [36] and refined by full-matrix least squares on F^2 using SHELXL-97 [37]. All non-hydrogen atoms were refined anisotropically. The carboxyl and water hydrogens were located from difference Fourier maps and the other hydrogens were placed in geometrically calculated positions. In **2**, the occupancy of the interstitial water O4 and O5 is 0.5. Crystal data and refinement parameters are listed in table 1.

3. Results and discussion

3.1. *Synthesis and structural descriptions*

Use of $PrCl_3$, $EuCl_3$ and $ErCl_3$ as the starting materials instead of Pr_2O_3, Eu_2O_3, and Er_2O_3, respectively, did not provide complexes **1–3**. Likewise, when $ZnCl_2$ and $CoCl_2$

Table 2. Selected bond lengths (Å) and angles (°) of **1–3**.

1		**2**		**3**	
Pr(1)–O(1)#1	2.372(4)	Eu(1)–O(1)	2.492(3)	Er(1)–O(1)	2.247(3)
Pr(1)–O(3)	2.526(3)	Eu(1)–O(6)	2.313(3)	Er(1)–O(3)	2.521(3)
Pr(1)–O(5)	2.375(3)	Eu(1)–O(8)	2.312(2)	Er(1)–O(5)	2.259(3)
Pr(1)–O(7)	2.545(4)	Eu(1)–O(10)	2.566(3)	Er(1)–O(7)	2.400(3)
Pr(1)–O(2)	2.462(2)	Eu(1)–O(2)	2.462(2)	Er(1)–O(2)#4	2.283(3)
Pr(1)–O(4)	2.309(3)	Eu(1)–O(7)#1	2.309(3)	Er(1)–O(4)	2.408(3)
Pr(1)–O(6)#2	2.416(4)	Eu(1)–O(9)#3	2.353(3)	Er(1)–O(6)#5	2.249(3)
Pr(1)–O(8)	2.520(3)	Eu(1)–O(11)	2.474(2)	Er(1)–O(8)	2.444(3)
O(2)–Pr(1)–O(3)	77.43(12)	O(1)–Eu(1)–O(2)	71.15(9)	O(1)–Er(1)–O(3)	79.04(12)
O(2)–Pr(1)–O(4)	74.59(16)	O(1)–Eu(1)–O(6)	75.62(11)	O(1)–Er(1)–O(4)	75.40(11)
O(2)–Pr(1)–O(5)	150.37(14)	O(1)–Eu(1)–O8	138.79(9)	O(1)–Er(1)–O(5)	150.71(12)
O(2)–Pr(1)–O(6)#2	77.69(18)	O(1)–Eu(1)–O(10)	129.54(9)	O(1)–Er(1)–O(7)	70.61(12)
O(2)–Pr(1)–O(7)	71.37(13)	O(1)–Eu(1)–O(11)	144.75(9)	O(1)–Er(1)–O(8)	139.19(12)
O(2)–Pr(1)–O(8)	137.47(15)	O(1)–Eu(1)–O(7)#1	70.44(9)	O(1)–Er(1)–O(6)#5	83.65(13)
O(1)#1–Pr(1)–O(2)	106.88(16)	O(1)–Eu(1)–O(9)#3	78.43(10)	O(1)–Er(1)–O(2)#4	106.69(12)
O(3)–Pr(1)–O(4)	50.32(10)	O(2)–Eu(1)–O(6)	80.84(10)	O(3)–Er(1)–O(4)	52.57(10)
O(3)–Pr(1)–O(5)	74.93(12)	O(2)–Eu(1)–O(8)	70.85(9)	O(3)–Er(1)–O(5)	74.45(12)
O(3)–Pr(1)–O(7)	146.00(13)	O(2)–Eu(1)–O(10)	145.75(9)	O(4)–Er(1)–O(7)	130.03(10)
O(3)–Pr(1)–O(8)	131.53(10)	O(2)–Eu(1)–O(11)	130.40(8)	O(4)–Er(1)–O(8)	143.69(12)
O(3)–Pr(1)–(6)#2	82.58(14)	O(2)–Eu(1)–O(7)#1	137.82(10)	O(4)–Er(1)–O(6)#5	130.35(12)
O(1)#1–Pr(1)–O(3)	127.90(14)	O(2)–Eu(1)–O(9)#3	76.42(11)	O(2)#4–Er(1)–O(4)	79.12(11)
O(4)–Pr(1)–O(5)	79.63(13)	O(6)–Eu(1)–O(8)	83.19(10)	O(5)–Er(1)–O(7)	138.21(12)
O(4)–Pr(1)–O(7)	129.28(11)	O(6)–Eu(1)–O(10)	79.73(9)	O(5)–Er(1)–O(8)	69.44(12)
O(4)–Pr(1)–O(8)	146.55(14)	O(6)–Eu(1)–O(11)	129.24(10)	O(5)–Er(1)–O(6)#5	103.38(12)
O(4)–Pr(1)–O(6)#2	129.14(15)	O(6)–Eu(1)–O(7)#1	105.61(11)	O(2)#4–Er(1)–O(5)	81.25(13)
O(1)#1–Pr(1)–O(4)	80.04(13)	O(6)–Eu(1)–O(9)#3	149.84(11)	O(7)–Er(1)–O(8)	71.76(11)
O(5)–Pr(1)–O(7)	137.90(13)	O(8)–Eu(1)–O(10)	79.04(10)	O(3)–Er(1)–O(7)	145.50(12)
O(5)–Pr(1)–O(8)	71.07(12)	O(8)–Eu(1)–O(11)	74.88(9)	O(3)–Er(1)–O(8)	129.23(11)
O(5)–Pr(1)–O(6)#2	108.80(14)	O(7)#1–Eu(1)–O(8)	150.39(9)	O(3)–Er(1)–O(6)#5	79.72(11)
O(1)#1–Pr(1)–O(5)	82.40(15)	O(8)–Eu(1)–O(9)#3	107.28(10)	O(2)#4–Er(1)–O(3)	128.86(11)
O(7)–Pr(1)–O(8)	70.31(12)	O(10)–Eu(1)–O(11)	51.68(8)	O(4)–Er(1)–O(5)	78.68(11)
O(6)#2–Pr(1)–O(7)	77.97(14)	O(7)#1–Eu(1)–O(10)	74.98(10)	O(6)#5–Er(1)–O(7)	80.97(12)
O(1)#1–Pr(1)–O(7)	75.31(15)	O(9)#3–Eu(1)–O(10)	129.48(10)	O(2)#4–Er(1)–O(7)	76.91(12)
O(6)#2–Pr(1)–O(8)	76.98(17)	O(7)#1–Eu(1)–O(11)	77.94(9)	O(6)#5–Er(1)–O(8)	75.40(13)
O(1)#1–Pr(1)–O(8)	80.42(13)	O(9)#3–Eu(1)–O(11)	80.89(10)	O(2)#4–Er(1)–O(8)	79.29(12)
O(1)#1–Pr(1)–O(6)#2	149.52(17)	O(7)#1–Eu(1)–O(9)#3	79.47(11)	O(2)#4–Er(1)–O(6)#5	150.51(13)

Symmetry operations: #1 $-x+1$, $-y+1$, $-z+1$; #2 $-x$, $-y+1$, $-z+1$; #3 $-x+2$, $-y+1$, $-z+1$; #4 $-x+1$, $-y+2$, $-z+1$; #5 $-x$, $-y+2$, $-z+1$.

Downloaded by [Renmin University of China] at 10:49 13 October 2013

were not added in the syntheses, crystals were not obtained. Both $ZnCl_2$ and $CoCl_2$ can in principle form complexes with the ligand, however, when only $ZnCl_2$ and $CoCl_2$ were added as the starting materials without any Ln_2O_3, no crystals were obtained. While the addition of $ZnCl_2$ and $CoCl_2$ may be responsible for the low yields of **1–3**, their presence is crucial for the production of crystalline material.

Crystallographic analysis revealed that **1–3** are isomorphous, so only the crystal structure of **2** is described here in detail. Selected bond lengths and angles are listed in table 2 and hydrogen bond data are listed in table 3. In **1–3**, HPA^- adopts two coordination modes, as shown in scheme 1.

3.2. *Crystal structure of 2*

In **2**, there are one crystallographicaly independent Eu^{3+}, three HPA^-, two coordinated and two lattice waters in the asymmetric unit, as shown in figure 1. The monodeprotonated HPA^- have three orientations; for convenience, HPA^- with N1, N3, and N5 (figure 1) are

Downloaded by [Renmin University of China] at 10:49 13 October 2013

Table 3. Geometrical hydrogen bonding parameters for **1–3**.

D–H···A	*d*(D–H) (Å)	*d*(H…A) (Å)	*d*(D…A) (Å)	∠DHA (°)
1				
O(7)–H(1 W)···O(9)	**0.85**	**1.97**	**2.82(7)**	**179.4**
O(7)–H(2 W)···O(11)	0.84	2.46	3.30(2)	169.7
O(8)–H(3 W)···O(3)#1	**0.83**	**2.12**	**2.72(5)**	**128.1**
O(8)–H(4 W)···O(9)	0.85	2.00	2.86(7)	178.9
O(9)–H(6 W)···N(4)#2	0.83	2.50	3.02(8)	120.0
N(3)–H(3D)···N(5)#3	**0.86**	**2.10**	**2.87(6)**	**148.7**
N(6)–H(6D)···N(4)#4	**0.86**	**2.36**	**3.14(6)**	**150.5**
Symmetry transformations used to generate equivalent atoms: #1 $-x, -y+1, -z+1$; #2 $x, y-1, z$; #3 $-x+1, -y+2, -z+1$; #4 $-x, -y+2, -z+1$				
2				
O(1)–H(1 W)···O(10)#1	0.83	1.93	2.75(4)	171.5
O(1)–H(2 W)···O(3)#1	0.83	2.03	2.82(4)	156.8
O(2)–H(4 W)···O(3)#1	**0.83**	**2.07**	**2.88(5)**	**164.2**
O(2)–H(3 W)···O(11)#2	0.83	**1.96**	2.75(3)	159.1
O(3)–H(6 W)···O(4)#3	0.85	1.83	2.68(13)	178.1
O(3)–H(5 W)···N(4)#4	0.83	2.20	3.01(5)	164.7
N(3)–H(3D)···N(5)#4	0.86	2.09	2.86(4)	149.6
N(6)–H(6D)···N(4)#5	0.86	2.37	3.14(5)	150.1
Symmetry transformations used to generate equivalent atoms: #1 $-x+1, -y+1, -z+1$; #2 $-x+2, -y+1, -z+1$; #3 $x-1, y, z$; #4 $-x+1, -y, -z+1$; #5 $-x+2, -y, -z+1$				
3				
O(7)–H(1 W)···O(4)#1	0.83	1.95	2.78(4)	171.2
O(7)–H(2 W)···O(9)#2	**0.83**	**2.07**	**2.87(6)**	**162.2**
O(8)–H(3 W)···O(9)#2	0.82	**2.08**	2.82(6)	149.4
O(8)–H(4 W)···O(3)#3	0.83	1.96	2.78(4)	171.0
O(9)–H(5 W)···N(2)	0.84	2.26	3.02(6)	151.8
O(9)–H(6 W)···O(10)	**0.85**	**1.84**	**2.69(19)**	**178.0**
O(10)–H(7 W)···O(10)#4	0.85	**2.11**	2.96(3)	178.0
O(10)–H(8 W)···O(9)	0.82	2.29	2.69(19)	110.1
O(11)–H(10 W)···O(12)#4	**0.84**	**2.14**	**2.94(3)**	**157.7**
O(12)–H(11 W)···O(11)#4	0.84	**2.22**	2.94(3)	143.1
O(12)–H(12 W)···O(10)	0.85	1.80	2.64(3)	169.1
N(1)–H(1D)···N(3)#5	0.86	2.08	2.85(5)	148.5
N(4)–H(4D)···N(2)#4	0.86	2.33	3.11(5)	150.7
Symmetry transformations used to generate equivalent atoms: #1 $-x+1, -y+2, -z+1$; #2 $x, y+1, z$; #3 $-x, -y+2, -z+1$; #4 $-x+1, -y+1, -z+1$; #5 $-x, -y+1, -z+1$				

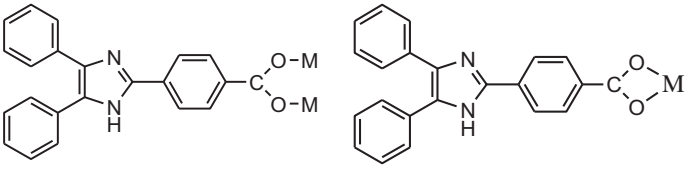

Scheme 1. Coordination modes of 4-(4,5-diphenyl-1H-imidazol-2-yl)benzoic acid in **1–3**.

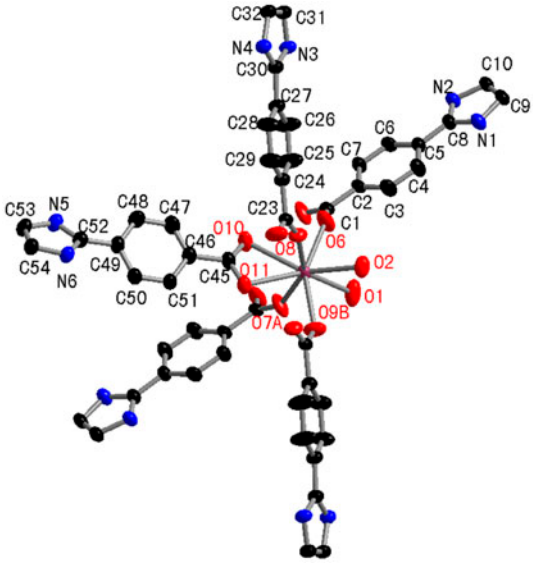

Figure 1. The coordination environment of Eu^{3+} in **2** with 50% probability thermal ellipsoids. All hydrogens and the two benzene rings on the imidazole ring are omitted for clarity.

named as HPA^a, HPA^b, and HPA^c, respectively. As shown in scheme 1, HPA^a and HPA^b adopt μ_2-bridging coordination, linking two Eu^{3+} cations with Eu···Eu distances of 4.908 and 4.810 Å, respectively, while HPA^c exhibits chelating coordination to one Eu^{3+}.

Eu^{3+} is coordinated to eight oxygens and displays a distorted triangular dodecahedral geometry. O1 and O2 are from two waters, O6, O7A, O8, O9B, O10, and O11 are from five HPA^-, of which carboxyl O6 and O7A are from two HPA^a, O8 and O9B are from two HPA^b, and the other two carboxyl oxygens (O10 and O11) are from one HPA^c. The Eu–O_{mc} (O_{mc}, monodentate carboxylate) bond lengths for O6, O7A, O8, and O9B are 2.313(3), 2.309(3), 2.312(2), and 2.353(3) Å, respectively, and the Eu–O_{cc} (O_{cc}, chelating carboxylate) bond lengths for O10 and O11 are 2.566(3) and 2.474(2) Å, respectively. The Eu–O_w (O_w, water) bond lengths for O1 and O2 are 2.492(2) and 2.462(3) Å, respectively. While Eu–O_{mc} bond lengths are essentially equivalent, there is a discernible difference in the Eu–O_{cc} bond lengths because the chelating carboxylate is asymmetrically bound. The average Eu–O_w bond length is longer than that of Eu–O_{mc}, but shorter than that of Eu–O_{cc}, and in general, the range of Eu–O bond lengths,

Downloaded by [Renmin University of China] at 10:49 13 October 2013

Downloaded by [Renmin University of China] at 10:49 13 October 2013

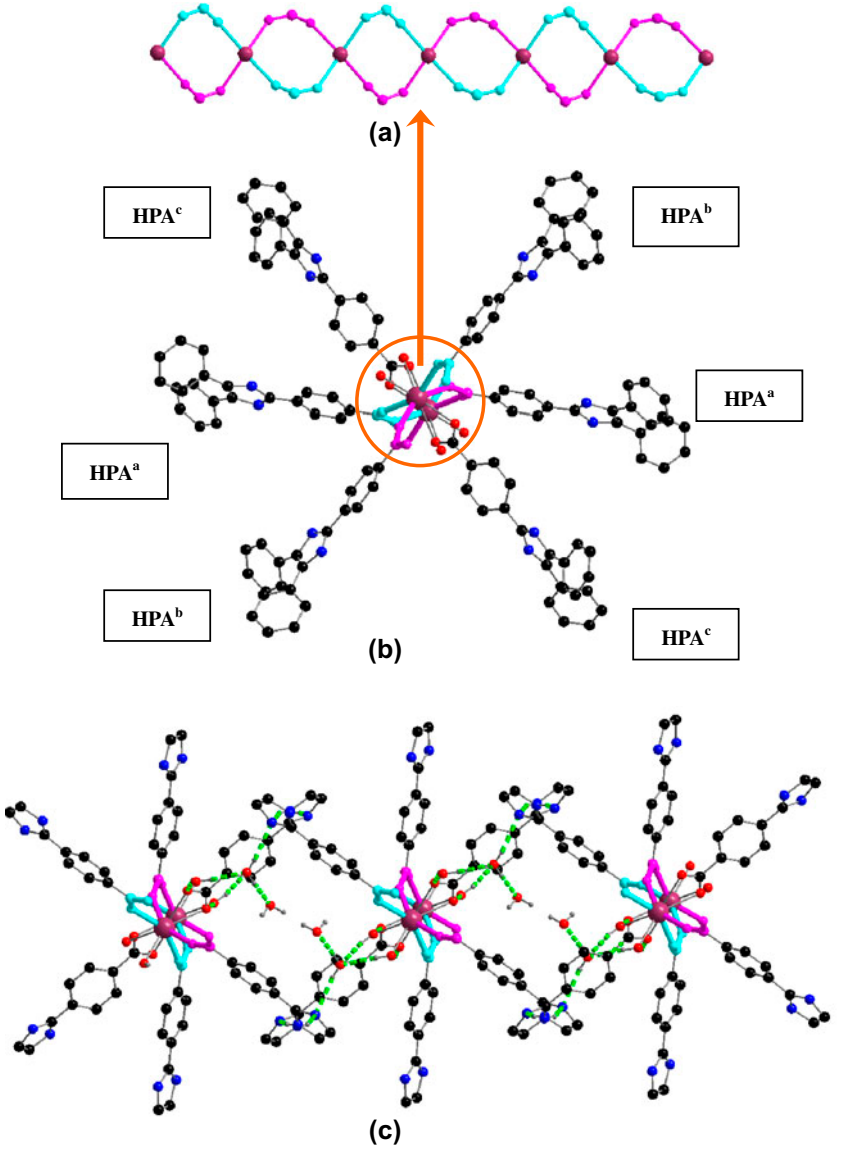

Figure 2. (a) View of the helical chain structure of **2** linked by carboxylates of HPA^a and HPA^b along the *b* axis; all the atoms except Eu^{3+} and the carboxylates of HPA^a and HPA^b are omitted for clarity; (b) view of the pinwheel structure of **2** along the *a*-axis; all the hydrogens are omitted for clarity; (c) view of the H-bonding connectivity among 1-D chains.

2.3–2.8 Å, are in accord with the values in previously reported Eu(III) complexes [38–40]. The chelating carboxylate angle, O_{cc}–Eu1–O_{cc}, is small, 51.68(7)°. The cisoid O–Eu–O angles are between 70.44(9) and 83.19(10)°, and the transoid O–Eu–O angles are between 129.24(10) and 150.39(9)°. The only exceptions are O6–Eu1–O7A and O8–Eu1–O9B angles, which are 105.61(11) and 107.28(10)°, respectively. All these

angles are within the range of those observed for Eu(III) complexes with O-donor ligands [41, 42].

HPA[a] and HPA[b] alternate along the Eu chain, linking Eu^{3+} cations into right and left helical chains united at Eu1 (figure 2(a)). The repeating unit can be described as $(–Eu1–O7–C1–O6–Eu1–O9–C23–O8–)_n$ and the pitch of the helix is the same as the length of the *a*-axis (9.576 Å). Viewed along the *a*-axis, every chain looks like a pinwheel (figure 2(b)). Eu^{3+} cations reside at the centers of the pinwheel, and the ligands fall into six groups, well arranged in six rows around the Eu^{3+}. Pinwheel structures [43–45] are not very common, however, the pinwheel structure of **2** is similar to lanthanide complexes with 2,2-diphenyldicarboxylate (dpdc) [43], where $[Eu_2(dpdc)_3(H_2O)_2]$ consists of two crystallographically independent Eu^{3+} ions with a Eu–Eu distance of 4.459 Å. Each dpdc bridges three Eu^{3+}, resulting in an infinite polymer chain, and every chain looks like a pinwheel when viewed along the *c* axis. Like **2**, the Eu^{3+} cations also reside at the center of the pinwheel and the dpdc ligands fall into three groups, well distributed around the Eu^{3+} centers.

There are multiple hydrogen bonds in **2** (table 3), including the O–H···O hydrogen bonds between coordinated water and carboxyl O of HPA[c] (O···O distances of 2.753 and 2.754 Å), O–H···O hydrogen bonds between waters (O···O distance of 2.667–2.816 Å), N–H···N hydrogen bonds between imidazole rings of HPA[b] and HPA[c] (N···N distances of 2.863 and 3.140 Å), and N–H···O hydrogen bonds between the imidazole ring of HPA[c] and a coordinated water. It is via these hydrogen bonds that the 1-D chain structures are constructed into a 2-D supramolecular structure. The Eu–Eu distance between the planes is 8.46 Å.

The mean Ln–O distances in **1–3** are 2.467, 2.410, and 2.351 Å, respectively, and decrease with increasing lanthanide atomic number, consistent with the lanthanide contraction [46].

3.3. *Powder X-ray diffraction and TG analysis of 2*

The experimental powder X-ray diffraction pattern of **2** (figure 3) closely matches that calculated from the single-crystal X-ray diffraction structure, indicating the phase purity of **2**.

The thermogravimetric (TG) curve of **2** exhibited two weight loss steps between 40 °C and 800 °C. The first weight loss of 6.1% from 40 to 103 °C corresponded to loss of four waters per asymmetric unit (Calcd: 5.8%). The compound was, thereafter, stable at 420 °C;

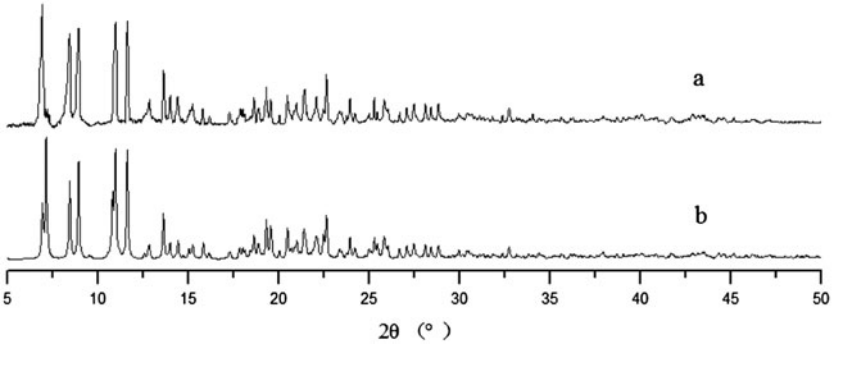

Figure 3. (a) Experimental PXRD pattern of **2**; (b) simulated PXRD of **2**.

Downloaded by [Renmin University of China] at 10:49 13 October 2013

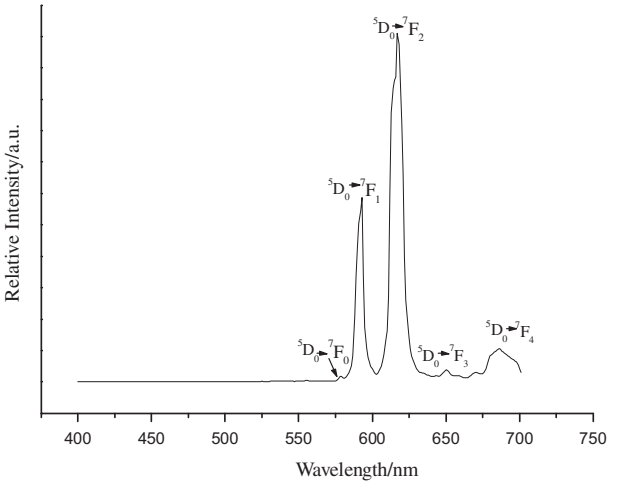

Figure 4. Emission spectrum of **2** corresponding to the $^5D_0 \rightarrow {}^7F_J$ ($J = 0$–4) transitions; $\lambda_{exc} = 385$ nm, $T = 293$ K.

the second weight loss of 65.4% (Calcd: 65.8%) occurred from 420 to 800 °C, corresponding to the removal of the organic groups and providing the final Eu_2O_3 residue.

3.4. *Fluorescence of 2*

Complex **2** emitted strong red light when excited by ultraviolet light. Figure 4 shows the luminescence spectrum of **2** excited with 385 nm light at 293 K. The five peaks in figure 4 correspond to $^5D_0 \rightarrow {}^7F_0$, $^5D_0 \rightarrow {}^7F_1$, $^5D_0 \rightarrow {}^7F_2$, $^5D_0 \rightarrow {}^7F_3$, and $^5D_0 \rightarrow {}^7F_4$ transitions of Eu^{3+}. The $^5D_0 \rightarrow {}^7F_2$ transition induced by the electric dipole is hypersensitive to the coordination environment of Eu^{3+}, while the $^5D_0 \rightarrow {}^7F_1$ transition is due to a magnetic dipole fairly insensitive to the environment of the cation. The intensity ratio, I ($^5D_0 \rightarrow {}^7F_2/{}^5D_0 \rightarrow {}^7F_1$) is ca. 1.72, which indicates that Eu^{3+} in **2** is not located at an inversion center and that the symmetry of Eu^{3+} is low [47].

4. Conclusion

Three new lanthanide supramolecular complexes with 4-(4,5-diphenyl-1H-imidazol-2-yl) benzoic acid have been synthesized and characterized. Ln^{3+} cations were bridged by HPA^- into a helical chain structure and the chains are further connected to a 2-D supramolecular structure by multiple hydrogen bonds. TG analysis of **2** showed that loss of water does not affect the thermal stability of **2**.

Supplementary material

Figures of the IR spectra for **1–3** and the TGA curve of **2**. The crystallographic data for the structures have been deposited with the Cambridge Crystallographic Data Center,

Downloaded by [Renmin University of China] at 10:49 13 October 2013

CCDC Nos. 902932–902934 for **1–3**. Copies of the data can be obtained free of charge on application to The Director, CCDC, 12 Union Road, Cambridge CB2 1EZ, UK (Fax: +44 1223 336 033; E-mail: deposit@ccdc.cam.ac.uk or www: http://www.ccdc.cam.ac.uk).

Acknowledgments

Financial support from the National Natural Science Foundation of China (Grant No. 21264011 and No. 20961007), the Bureau of Education of Jiangxi Province (Grant No. GJJ09064) and the State Key Laboratory of Food Science and Technology of Nanchang University (No. SKLF-TS-200915) are gratefully acknowledged.

Downloaded by [Renmin University of China] at 10:49 13 October 2013

References

[1] K.S. Min, A.G. DiPasquale, J.A. Golen, A.L. Rheingold, J.S. Miller. *J. Am. Chem. Soc.*, **129**, 2360 (2007).
[2] S. Patil, J. Claffey, A. Deally, M. Hogan, B. Gleeson, L.M.M. Méndez, H. Müller-Bunz, F. Paradisi, M. Tacke. *Eur. J. Inorg. Chem.*, **7**, 1020 (2010).
[3] G. Consiglio, S. Failla, P. Finocchiaro, I.P. Oliveri, R. Purrello, S.D. Bella. *Inorg. Chem.*, **49**, 5134 (2010).
[4] L. Qin, J.S. Hu, L.F. Huang, Y.Z. Li, Z.J. Guo, H.G. Zheng. *Cryst. Growth Des.*, **10**, 4176 (2010).
[5] Y. Chen, C.B. Liu, Y.N. Gong, J.M. Zhong, H.L. Wen. *Polyhedron*, **36**, 6 (2012).
[6] X.J. Zheng, T.T. Zheng, L.P. Jin. *J. Mol. Struct.*, **740**, 31 (2005).
[7] Y.N. Gong, C.B. Liu, H.L. Wen, L.S. Yan, Z.Q. Xiong, L. Ding. *New J. Chem.*, **35**, 865 (2011).
[8] C.B. Liu, L. Xiang, X.X. Li, H.L. Wen. *Chem. J. Chin. Univ.*, **27**, 2256 (2006).
[9] S.Q. Zhang, F.L. Jiang, M.Y. Wu, R. Feng, J. Ma, W.T. Xu, M.C. Hong. *Inorg. Chem. Commun.*, **14**, 1400 (2011).
[10] D.C. Zhong, M. Meng, J. Zhu, G.Y. Yang, T.B. Lu. *Chem. Commun.*, **46**, 4354 (2010).
[11] J.G. Lombardino, E.H. Wiseman. *J. Med. Chem.*, **17**, 1182 (1974).
[12] O.L. Heinrich, L.B. Hans, D.B. Uwe. US 6 451 520 B1 (2002).
[13] S. Mataka, T. Hatta. WO 085 208 A1 (2005).
[14] S. Park, O.H. Kwon, S. Kim, S. Park, M.G. Choi, M. Cha. *J. Am. Chem. Soc.*, **127**, 10070 (2005).
[15] W.L. Pan, H.B. Tan, Y. Chen, D.H. Hu, H.B. Liu, Y.Q. Wan, H.C. Hong. *Dyes Pigm.*, **76**, 17 (2008).
[16] J. Santos, E.A. Mintz, O. Zehnder, C. Bosshard, X.R. Bu, P. Günter. *Tetrahedron Lett.*, **42**, 805 (2001).
[17] C.F. Lee, C.Y. Liu, H.C. Song, T.Y. Luh. *Chem. Commun.*, **41**, 2821 (2002).
[18] D. Yanover, M. Kaftory. *Acta Cryst.*, **E65**, o711 (2009).
[19] D.C. Braddock, S.A. Hermitage, J.M. Redmond, A.J.P. White. *Tetrahedron: Asymmetry*, **17**, 2935 (2006).
[20] X.F. Huang, Y.M. Song, X.S. Wang, J. Pang, J.L. Zuo, R.G. Xiong. *J. Organomet. Chem.*, **691**, 1065 (2006).
[21] L. Benisvy, A.J. Blake, D. Collison, E.S. Davies, C.D. Garner, E.J.L. Mclnnes, J. McMaster, G. Whittaker, C. Wilson. *Chem. Commun.*, **18**, 1824 (2001).
[22] L. Benisvy, A.J. Blake, D. Collison, E.S. Davies, C.D. Garner, E.J.L. Mclnnes, J. McMaster, G. Whittaker, C. Wilson. *Dalton Trans.*, 1975 (2003).
[23] L. Benisvy, E. Bill, A.J. Blake, D. Collison, E.S. Davies, C.D. Garner, G. McArdle, E.J.L. Mclnnes, J. McMaster, S.H.K. Ross, C. Wilson. *Dalton Trans.*, 258 (2006).
[24] H.L. Wen, T.T. Wang, C.B. Liu, M. He, Y.X. Wang. *J. Coord. Chem.*, **65**, 856 (2012).
[25] B. Saha, S. Chakraborty, G. Das. *J. Phys. Chem. C*, **114**, 9817 (2010).
[26] J.A. Danis, M.R. Lin, B.L. Scott, B.W. Eichhorn, W.H. Runde. *Inorg. Chem.*, **40**, 3389 (2001).
[27] R.M. LoPachin, T. Gavin, A. DeCaprio, D.S. Barber. *Chem. Res. Toxicol.*, **25**, 239 (2012).
[28] R.Y. Wang, Z.P. Zheng, T.Z. Jin, R.J. Staples. *Angew. Chem. Int. Ed.*, **38**, 1813 (1999).
[29] Y. Cui, H.L. Ngo, P.S. White, W. Lin. *Chem. Commun.*, **16**, 1666 (2002).
[30] C.B. Liu, H.L. Wen, S.S. Tan, X.G. Yi. *J. Mol. Struct.*, **879**, 25 (2008).
[31] D. Weng, X. Zheng, L. Jin. *Eur. J. Inorg. Chem.*, **20**, 4184 (2006).
[32] M. Kidwai, P. Mothsra, V. Bansal, R.K. Somvanshi, A.S. Ethayathulla, S. Dey, T.P. Singh. *J. Mol. Catal. A: Chem.*, **265**, 177 (2006).
[33] Y. Ogata, A. Kawasaki, F. Sugiura. *J. Org. Chem.*, **34**, 3981 (1969).
[34] L.M. Wang, Y.H. Wang, H. Tian, Y.F. Yao, J.H. Shao, B. Liu. *J. Fluorine Chem.*, **127**, 1570 (2006).
[35] G.M. Sheldrick. *SADABS, Program for Empirical Absorption Correction of the Area Detector Data*, University of Göttingen, Germany (1997).

[36] G.M. Sheldrick. *SHELXL-97, Program for Crystal Structure Solution*, University of Göttingen, Germany (1997).
[37] G.M. Sheldrick. *SHELXL-97, Program for Crystal Structure Refinement*, University of Göttingen, Germany (1997).
[38] Z.H. Wang, J. Fan, W.G. Zhang. *Z. Anorg. Allg. Chem.*, **635**, 2333 (2009).
[39] J. Fan, Z.H. Wang, M. Yang, X. Yin, W.G. Zhang, Z.F. Huang, R.H. Zeng. *Cryst. Eng. Commun.*, **12**, 216 (2010).
[40] J. Wang, J. Fan, L.Y. Guo, X. Yin, Z.H. Wang, W.G. Zhang. *J. Solid State Chem.*, **183**, 575 (2010).
[41] D.K. Cao, S.Z. Hou, Y.Z. Li, L.M. Zheng. *Cryst. Growth Des.*, **9**, 4445 (2009).
[42] S. Chen, R.-Q. Fan, C.-F. Sun, P. Wang, Y.-L. Yang, Q. Su, Y. Mu. *Cryst. Growth Des.*, **12**, 1337 (2012).
[43] Y.-B. Wang, X.-J. Zheng, W.-J. Zhuang, L.-P. Jin. *Eur. J. Inorg. Chem.*, **19**, 1355 (2003).
[44] R. Horinkoshi, C. Nambu, T. Mochida. *Inorg. Chem.*, **42**, 6868 (2003).
[45] R. Wang, R. Li, Y. Bian, C.-F. Choi, D.K.P. Ng, J. Dou, D. Wang, P. Zhu, C. Ma, R.D. Hartnell, D.P. Arnold, J. Jiang. *Chem. Eur. J.*, **11**, 7351 (2005).
[46] C.-B. Liu, X.-J. Zheng, Y.-Y. Yang, L.-P. Jin. *Inorg. Chem. Commun.*, **8**, 1045 (2005).
[47] J.-C.G. Bünzli, G.R. Choppin. *Lanthanide Probes in Life, Chemical and Earth Sciences: Theory and Practice*, Elsevier, Amsterdam (1989).

Downloaded by [Renmin University of China] at 10:49 13 October 2013